

**This is an electronic reprint of the original article.
This reprint *may differ* from the original in pagination and typographic detail.**

Author(s): Mikheenko, P.; Vestgårdén, J. I.; Chaudhuri, Saumyadip; Maasilta, Ilari; Galperin, M.;
Johansen, T. H.

Title: Metal frame as local protection of superconducting films from thermomagnetic
avalanches

Year: 2016

Version:

Please cite the original version:

Mikheenko, P., Vestgårdén, J. I., Chaudhuri, S., Maasilta, I., Galperin, M., & Johansen,
T. H. (2016). Metal frame as local protection of superconducting films from
thermomagnetic avalanches. *AIP Advances*, 6, Article 035304.
<https://doi.org/10.1063/1.4943549>

All material supplied via JYX is protected by copyright and other intellectual property rights, and duplication or sale of all or part of any of the repository collections is not permitted, except that material may be duplicated by you for your research use or educational purposes in electronic or print form. You must obtain permission for any other use. Electronic or print copies may not be offered, whether for sale or otherwise to anyone who is not an authorised user.



Metal frame as local protection of superconducting films from thermomagnetic avalanches

P. Mikheenko, J. I. Vestgård, S. Chaudhuri, I. J. Maasilta, Y. M. Galperin, and T. H. Johansen

Citation: *AIP Advances* **6**, 035304 (2016); doi: 10.1063/1.4943549

View online: <http://dx.doi.org/10.1063/1.4943549>

View Table of Contents: <http://scitation.aip.org/content/aip/journal/adva/6/3?ver=pdfcov>

Published by the *AIP Publishing*

Articles you may be interested in

[Limiting thermomagnetic avalanches in superconducting films by stop-holes](#)

Appl. Phys. Lett. **103**, 032604 (2013); 10.1063/1.4813908

[Thermo-magnetic stability of superconducting films controlled by nano-morphology](#)

Appl. Phys. Lett. **102**, 252601 (2013); 10.1063/1.4812484

[Nanosecond voltage pulses from dendritic flux avalanches in superconducting NbN films](#)

Appl. Phys. Lett. **102**, 022601 (2013); 10.1063/1.4775693

[Superconductivity of 80 Nb N – 20 Si O 2 granular films](#)

Low Temp. Phys. **36**, 1058 (2010); 10.1063/1.3533238

[Avalanche-driven fractal flux distributions in NbN superconducting films](#)

Appl. Phys. Lett. **87**, 042502 (2005); 10.1063/1.1992673

The image shows the cover of an AIP Applied Physics Reviews journal issue. The cover features a blue and orange color scheme with a molecular structure background. The text 'NEW Special Topic Sections' is prominently displayed in white. Below this, it says 'NOW ONLINE' and 'Lithium Niobate Properties and Applications: Reviews of Emerging Trends'. The AIP Applied Physics Reviews logo is in the bottom right corner.

NEW Special Topic Sections

NOW ONLINE
Lithium Niobate Properties and Applications:
Reviews of Emerging Trends

AIP Applied Physics Reviews

Metal frame as local protection of superconducting films from thermomagnetic avalanches

P. Mikheenko,^{1,a} J. I. Vestgården,^{1,2} S. Chaudhuri,³ I. J. Maasilta,³
Y. M. Galperin,^{1,4} and T. H. Johansen^{1,5}

¹*Department of Physics, University of Oslo, P.O. Box 1048 Blindern, 0316 Oslo, Norway*

²*Norwegian Defence Research Establishment (FFI), P.O.Box 25, NO-2027 Kjeller, Norway*

³*Nanoscience Center, Department of Physics, P.O. Box 35, University of Jyväskylä, FIN-40014 Jyväskylä, Finland*

⁴*Physico-Technical Institute RAS, 26 Politekhnicheskaya, St Petersburg 194021 St. Petersburg, Russian Federation*

⁵*Institute for Superconducting and Electronic Materials, University of Wollongong, Innovation Campus, Squires Way, North Wollongong, NSW 2500, Australia*

(Received 18 December 2015; accepted 25 February 2016; published online 4 March 2016)

Thermomagnetic avalanches in superconducting films propagating extremely fast while forming unpredictable patterns, represent a serious threat for the performance of devices based on such materials. It is shown here that a normal-metal frame surrounding a selected region inside the film area can provide efficient protection from the avalanches during their propagation stage. Protective behavior is confirmed by magneto-optical imaging experiments on NbN films equipped with Cu and Al frames, and also by performing numerical simulations. Experimentally, it is found that while conventional flux creep is not affected by the frames, the dendritic avalanches are partially or fully screened by them. The level of screening depends on the ratio of the sheet conductance of the metal and the superconductor in the resistive state, and for ratios much larger than unity the screening is very efficient. © 2016 Author(s). All article content, except where otherwise noted, is licensed under a Creative Commons Attribution (CC BY) license (<http://creativecommons.org/licenses/by/4.0/>). [<http://dx.doi.org/10.1063/1.4943549>]

The number of applications based on superconductors increases, and with the important role these devices will play in technology,¹⁻³ safe operation becomes crucially important. When loaded with a high electrical current, or exposed to a strong magnetic field, the superconductors accumulate large amounts of energy. This energy can suddenly be released through a thermomagnetic runaway, or avalanche, which in general is very harmful, e.g., to superconducting magnets and electronic devices. Especially vulnerable are superconducting thin-film devices experiencing a perpendicular magnetic field, where avalanche events may occur at fields as low as a few millitesla.^{4,5}

The instability that triggers such avalanches is deeply rooted in the nature of type-II superconductors, where magnetic flux exists in the form of quantized vortices. If a vortex moves, it dissipates energy causing a local temperature rise in the material. This promotes motion of the neighboring vortices, and the positive feedback can create a massive thermomagnetic avalanche. In thin films, magneto-optical imaging⁶ (MOI) has revealed that the instability leads to abrupt flux motion in the form of large, often sample-spanning, dendritic structures, where each branch propagates at a speed up to 100 km/s.⁷⁻⁹ The phenomenon has been observed in films of many superconducting materials.^{7,10-15}

Although the avalanche behavior has already undergone extensive investigations,¹⁶ one finds from a practical viewpoint that these events are largely out of control. Partly, this is due to (i) the unpredictability of when and where an avalanche starts, and (ii) the unpredictable path that each

^aElectronic mail: pavlo.mikheenko@fys.uio.no

branch of the avalanche will follow. Furthermore, experimental studies of the phenomenon are severely limited by the lack of techniques allowing to investigate the flux dynamics on the relevant time scale of a few nanoseconds. This is the duration of a typical event,¹⁷ and is also the time scale when damage is done to a device. In fact, an avalanche can permanently damage the superconductor, as shown in recent work on $\text{YBa}_2\text{Cu}_3\text{O}_x$ films.¹⁸ Here, MOI revealed that superconducting properties can be lost in parts of the avalanche path, and atomic force microscopy scans showed that the local heating can even cause complete disintegration of the material. Thus, from an applied perspective it is essential to find means to prevent such events from happening, in particular, in regions of vital importance for the functionality of a device.

Previous experiments demonstrated that a uniform metal layer deposited on the superconducting film can suppress the avalanche activity.^{19–23} The screening comes from the very high speed of the propagating flux dendrites, which when hitting the metal induce eddy currents by extracting energy from the avalanche. It was also reported that one may selectively prevent avalanche nucleation along the rim by coating parts of it with a normal metal film.^{24,25} In the present work, we show that avalanches can be stopped even after they have nucleated, i.e., during their fast and destructive propagation stage. This is done by adding a normal metal frame surrounding a selected internal area of the superconducting film. The efficiency of the local protection is documented by MOI observations and numerical simulations.

The sample configuration chosen in this work is a square superconducting film, see Fig. 1, where in the central part a narrow square metal frame (light brown color) is placed to protect the area it surrounds. The figure illustrates the result of a numerical simulation where such a sample is exposed to an increasing perpendicular magnetic field. The numerical procedure solves the Maxwell equations coupled with the heat flow equation for a thin-film conductor experiencing a transverse applied magnetic field, as described in Ref. 26. The electromagnetic braking-effect is included in the model by treating the two layers as conductors connected in parallel.²⁷ The braking is quantified by the parameters S , which is the ratio of the conductance of the two layers when both are in the normal state.²⁸

In the figure the film edge appears as a very bright contour, showing the piling up of the external field due to the diamagnetic response of the superconductor. This particular image represents the flux density at a time 65 ns after an avalanche started from the upper film edge. Evidently,



FIG. 1. Numerical simulation of the flux distribution in a superconducting film, where the propagation of an avalanche was blocked by a metal frame (light-brown). The brightness of the green color represents the magnitude of the flux density.

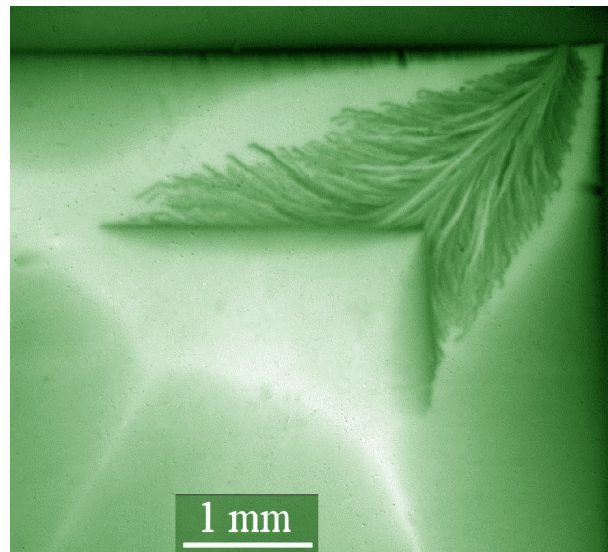


FIG. 2. Flux distribution in the upper right corner area of a NbN film, as the descending field reaches 9.2 mT. The magneto-optical image was recorded using slightly uncrossed polarizers.

this avalanche propagated in a branched fashion, and the shown dendritic structure is the final flux pattern after the avalanche came to rest. The spatially smooth penetration of flux from all the external edges shows the regular behavior of a square superconducting film.

From the flux distribution in Fig. 1 it is clear that the avalanche was strongly influenced by the metal frame. Indeed, the frame fully prevented all the rapidly approaching flux branches from entering the enclosed central region. Interestingly, this protection occurs in two different ways, namely (i) by reflecting incoming flux branches, and (ii) by damping the flux motion taking place under the metal coating. Note also that in the upper horizontal part of the metal frame, the flux branches hitting the frame at approximately normal incidence are close to penetrate through the obstruction. Also the right vertical part of the frame is activated, serving to guide some branches along the outer edge of the frame.

To test in practice the avalanche-protection ability of a metal frame on superconducting films, pulsed laser deposition was used to grow films of NbN on MgO (001) single crystal substrates.²⁹ A film of thickness 170 nm was shaped as a square with sides measuring 8 mm. A $1\ \mu\text{m}$ thick Cu frame was then deposited directly on the sample, with the same relative positioning as seen in Fig. 1. Before the deposition sample was exposed to the air, so one expects a formation of natural oxide layer between Cu and NbN. The square frame measures 4 mm externally, and has a width of 0.5 mm. Visualization of magnetic flux distributions across the sample area was done by MOI using a Faraday rotating ferrite garnet sensor plate^{30,31} placed directly on the sample.

Shown in Fig. 2 is a magneto-optical image of the flux distribution formed by an avalanche starting from the upper edge of an NbN film. The sample had here first been zero-field-cooled to 4 K, and then exposed to a 12 mT perpendicular field, which caused full penetration of flux without triggering any avalanche. The applied field was then reduced, and when reaching 9.2 mT the dendritic avalanche seen in the figure occurred.

It is evident that all the branches in this avalanche were blocked by the metal frame. Interestingly, the blocking has to a large extent the character of reflection from the interface.²⁵ Another visible feature is that some of the avalanching flux, when hitting the frame, penetrates smoothly into the metal coated area, where it finally comes to rest in a critical-state-like distribution. The frame gives here full avalanche protection of the enclosed area, and does it with characteristics agreeing very well with the simulation results.

When lowering the applied field further to 5.8 mT, a second avalanche occurred, starting from a different point on the upper sample edge, see Fig. 3. The new starting point caused many of the

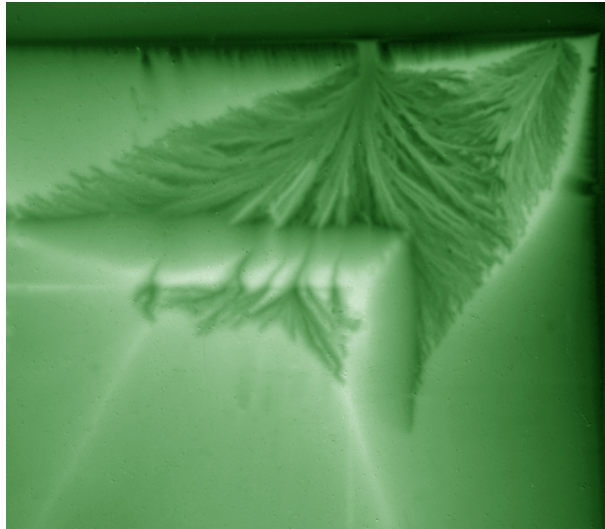


FIG. 3. Magnetic flux distribution as in Fig. 2 when the field is further reduced to 5.8 mT. When a second, more powerful, avalanche occurs, the protection is incomplete.

branches in the avalanche to hit the frame at near perpendicular incidence. Evidently, some of these branches traverse the frame. Although they leave only faint traces of their crossing, they form again a typical branched patterns when entering the uncoated square. Thus, in this case the metal frame was not able to provide full protection of the central area. This is a typical behaviour observed in many more avalanche events. The experiments also reveal that the penetration of avalanche branches into the framed region depends on the angle of incidence. Avalanche branches hitting the frame at near normal incidence are much less screened than those hitting at smaller angles which are mostly reflected.

To verify the importance of the angle between the metal frame edge and the direction of the incoming avalanche branches, simulations were performed with an indentation at the edge causing the avalanche to start from a geometrical location similar to what is seen in Fig. 3. The result of the numerical calculation is shown in Fig. 4. The key features of the experimental and numerical



FIG. 4. Simulated penetration of a dendrite through the conductive frame. $S = 10$.

results are again strikingly similar, in particular the fact that several branches of the avalanche are now traversing the metal frame. Moreover, the branches entering the area to be protected are seen to form further branching.

According to Ref. 28 the electromagnetic damping of thermomagnetic avalanches by a normal-metal coating is governed by the dimensionless parameter, $S = (\rho_s d_m)/(\rho_m d_s)$. Here, ρ_m and ρ_s are resistivities of the metal and superconductor (in the resistive state), respectively, while d_m and d_s are the thicknesses of the corresponding layers. In other words, S is the ratio of the normal-state sheet resistance of the superconductor, R_s , and the sheet resistance of the coating metal, R_m . For efficient screening the value of S should be much larger than unity. In the present case R_s and R_m were found after subtracting the contact resistance, which was extracted from data obtained for different distances between the leads. We found that at room temperature R_s between points separated by 2.25 mm equals 7 Ohm, while R_m between the points separated by the same distance is 0.5 Ohm. This gives $S \approx 14$ for the sample displayed in Figs. 2 and 3, quite consistent with the fairly good avalanche protection.

An obvious way to increase the screening efficiency is to increase the thickness of the normal metal layer. However, deposition of a layer with thickness much more than one micron is difficult since thick metal films tend to peel off the sample. Also due to a finite skin depth in the metal at the ultra-short time scale typical for the dendrite propagation, only part of the thickness could contribute to screening. For example, the skin depth in Al is $\sim 2 \mu\text{m}$ for processes of duration of 1 ns, and $6 \mu\text{m}$ for processes with a characteristic time of 10 ns.

A more reliable and flexible approach could be to use an external frame rather than one deposited on the film. To test this concept, a frame was made from a $13 \mu\text{m}$ thick Al technical foil. The frame was prepared by mechanically cutting the foil under an optical microscope using a specially designed tool. The frame measured 1.5 mm and 1.7 mm externally, and was 0.45 mm wide. It was placed on the superconductor using the light pressure from the magneto-optical sensor plate for stable mounting.

Shown in Fig. 5 is the observed flux penetration pattern inside the sample after it was initially zero-field cooled to 4 K, and then subjected to a perpendicular field of 2.9 mT. Panel a) displays the magneto-optical image using color coding, where red color represents its maximum brightness. The frame is indicated by the black dashed lines showing a slight rotation relative to the superconductor square.

In this figure, as in Fig. 3, one sees two regimes of flux penetration – one consisting of avalanche dendrites, and one showing conventional penetration forming typical critical-state profiles.³² The avalanching flux is again strongly influenced by the frame, which prevents nearly all the incoming branches from entering into the central uncoated area. Instead, they disperse into a smooth flux distribution within the metal-coated part. Only one small fragment of the flux branches reaches the central frame area. Contrary, one sees that the flux having penetrated the sample from the lower left side of the square, was not at all influenced by the metal frame as it entered the frame area at a much smaller velocity. Also, our numerical simulations show that slowly driven flux penetration as well as thermally activated creep, are not influenced by a metal layer, as the eddy currents induced in these cases are negligible.

The magneto-optical image in Fig. 5(a) was recalculated^{33,34} into a distribution of the flux density, B over the sample area. The panel b) displays the flux density along the white line drawn in panel a). From the B -profile one sees that the area enclosed by the frame has a large continuous region of perfect screening. Thus, if a sensitive superconducting device were placed there, it would not be affected by the avalanche event. Note also that due to the finite skin depth, there is little to gain by increasing the thickness of this frame any further. However, improving the quality of the Al-foil and its mounting is likely to make the screening more efficient.

Interestingly, one can see from panel b) that the B -profile across the frame is substantially steeper than the Bean critical-state profile in the bare sample. Therefore, coating by a normal metal improves the screening of fast electromagnetic excitations in type-II superconductors. Overall, with the deposition of a highly conductive normal metal layer and proper adjustment of the device geometry, one can obtain substantial screening of dendritic avalanches, the propagation of slowly moving magnetic flux remaining essentially unperturbed.

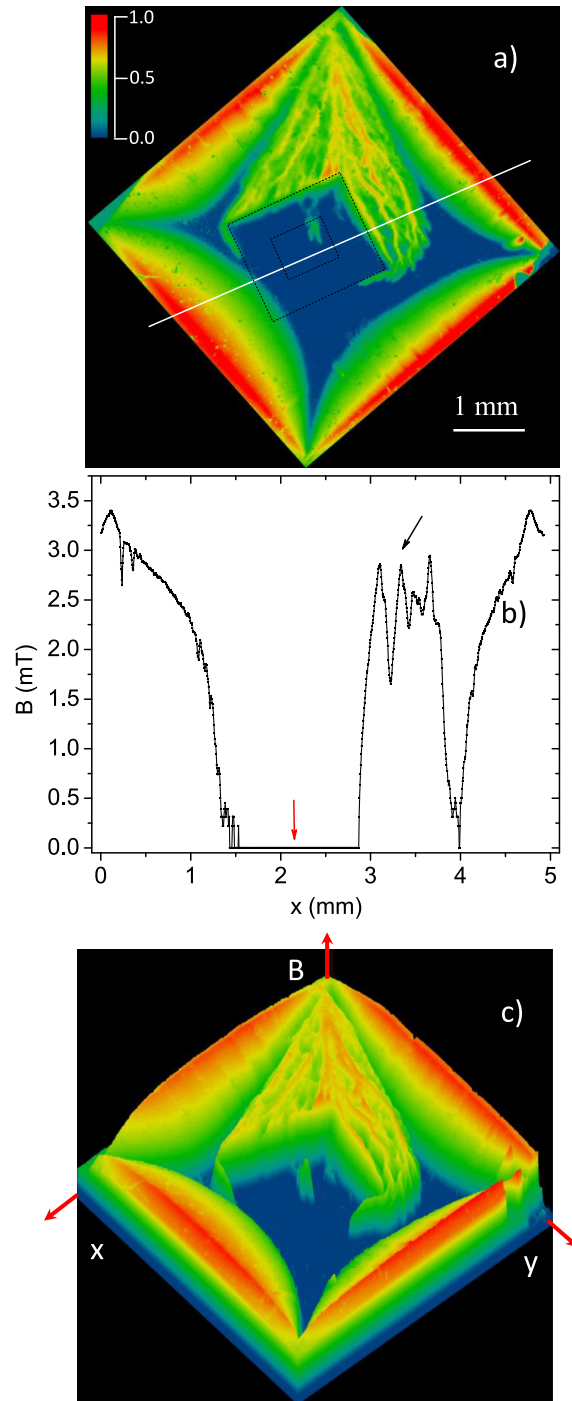


FIG. 5. a) A color-coded magneto-optical image of superconducting film with an Al frame (see the dark dotted lines) in an applied magnetic field of 2.9 mT. The numbers at the scale correspond to the image brightness in arbitrary units. b) The local magnetic field profile along the white line shown in a). c) A 3D representation of the flux density in the sample.

In conclusion, it is demonstrated that a normal metal frame added on top of a superconducting film strongly impedes the propagation of thermomagnetic avalanches. Using such frames, it is possible to screen selected areas of the film from the destructive avalanche events, while keeping unaffected all slowly moving magnetic flux, e.g., as part of the communication with superconducting electronics located inside the area enclosed by the frame.

- ¹ John Sarrao (Chairman), *Basic Research Needs for Superconductivity* (Office of Science, U.S. Department of Energy, 2006).
- ² Y. Wang, *Fundamental Elements of Applied Superconductivity in Electrical Engineering* (John Wiley & Sons, Inc, 2013).
- ³ P. Mikheenko, *Journal of Physics: Conference Series* **286**, 012014 (2011).
- ⁴ T. H. Johansen, M. Baziljevich, D. V. Shantsev, P. E. Goa, Y. M. Galperin, W. N. Kang, H. J. Kim, E. M. Choi, M.-S. Kim, and I. Lee, *EPL* **59**, 599 (2002).
- ⁵ D. V. Shantsev, A. V. Bobyl, Y. M. Galperin, T. H. Johansen, and S. I. Lee, *Phys. Rev. B* **72**, 024541 (2005).
- ⁶ M. V. Indenbom, T. Schuster, M.R. Koblishka, A. Forkl, H. Kronmüller, L. A. Dorosinsku, V. K. Vlasko-Vlasov, A. A. Polyanskii, R. L. Prozorov, and V. I. Nikitenko, *Physica C* **209**, 259 (1993).
- ⁷ P. Leiderer, J. Boneberg, P. Brüll, V. Bujok, and S. Herminghaus, *Phys. Rev. Lett.* **71**, 2646 (1993).
- ⁸ U. Bolz, B. Biehler, D. Schmidt, B. Runge, and P. Leiderer, *EPL* **64**, 517 (2003).
- ⁹ U. Bolz, D. Schmidt, B. Biehler, B. Runge, R. G. Mints, K. Numssen, H. Kinder, and P. Leiderer, *Physica C* **388–399** (2003).
- ¹⁰ C. A. Durán, P. L. Gammel, R. E. Miller, and D. J. Bishop, *Phys. Rev. B* **52**, 75 (1995).
- ¹¹ T. H. Johansen, M. Baziljevich, D. V. Shantsev, P. E. Goa, Y. M. Galperin, W. N. Kang, H. J. Kim, E. M. Choi, M.-S. Kim, and S. I. Lee, *Supercond. Sci. Technol.* **14**, 726 (2001).
- ¹² I. A. Rudnev, S. V. Antonenko, D. V. Shantsev, T. H. Johansen, and A. E. Primenko, *Cryogenics* **43**, 663 (2003).
- ¹³ E. Altshuler, T. H. Johansen, Y. Paltiel, P. Jin, K. E. Bassler, O. Ramos, Q. Y. Chen, G. F. Reiter, E. Zeldov, and C. W. Chu, *Phys. Rev. B* **70**, 140505 (2004).
- ¹⁴ S. C. Wimbush, B. Holzappel, and Ch. Jooss, *J. App. Phys.* **96**, 3589 (2004).
- ¹⁵ I. A. Rudnev, D. V. Shantsev, T. H. Johansen, and A. E. Primenko, *Appl. Phys. Lett.* **87**, 042502 (2005).
- ¹⁶ E. Altshuler and T. H. Johansen, *Rev. Mod. Phys.* **76**, 471 (2004).
- ¹⁷ J. I. Vestgård, D. V. Shantsev, Y. M. Galperin, and T. H. Johansen, *Sci. Rep.* **2**, 886 (2012).
- ¹⁸ M. Baziljevich, E. Baruch-El, T. H. Johansen, and Y. Yeshurun, *Appl. Phys. Lett.* **105**, 012602 (2014).
- ¹⁹ M. Baziljevich, A. V. Bobyl, D. V. Shantsev, E. Altshuler, T. H. Johansen, and S. I. Lee, *Physica C* **369**, 93 (2002).
- ²⁰ E.-M. Choi *et al.*, H.-S. Lee, H. J. Kim, B. Kang, S. Lee, Å. A. F. Olsen, D. V. Shantsev, and T. H. Johansen, *Appl. Phys. Lett.* **87**, 152501 (2005).
- ²¹ J. Albrecht, A. T. Matveev, M. Djupmyr, G. Schütz, B. Stuhlhofer, and H. Habermeier, *Appl. Phys. Lett.* **87**, 182501 (2005).
- ²² S. Treiber and J. Albrecht, *New Journal of Physics* **12**, 093043 (2010).
- ²³ J. Brisbois, B. Vanderheyden, F. Colauto, M. Motta, W. A. Ortiz, J. Fritzsche, N. D. Nguyen, B. Hackens, O.-A. Adami, and A. V. Silhanek, *New J. Phys.* **16**, 103003 (2014).
- ²⁴ E.-M. Choi, V. V. Yurchenko, T. H. Johansen, H.-S. Lee, J. Y. Lee, W. N. Kang, and S.-I. Lee, *Supercond. Sci. Technol.* **22** (2009).
- ²⁵ P. Mikheenko, T. H. Johansen, S. Chaudhuri, I. Maasilta, and Y. M. Galperin, *Phys. Rev. B* **91**, 060507(R) (2015).
- ²⁶ J. I. Vestgård, P. Mikheenko, Y. M. Galperin, and T. H. Johansen, *New J. Phys.* **15**, 093001 (2013).
- ²⁷ J. I. Vestgård, Y. M. Galperin, and T. H. Johansen, *J. Low Temp. Phys.* **173**, 303 (2013).
- ²⁸ J. I. Vestgård, P. Mikheenko, Y. M. Galperin, and T. H. Johansen, *Supercond. Sci. Technol.* **27**, 055014 (2014).
- ²⁹ S. Chaudhuri, M. R. Nevala, T. Hakkarainen, T. Niemi, and I. J. Maasilta, *IEEE Transactions on Applied Superconductivity* **21**, 143 (2011).
- ³⁰ L. E. Helseth, R. W. Hansen, E. I. Il'yashenko, M. Baziljevich, and T. H. Johansen, *Phys. Rev. B* **64**, 174406 (2001).
- ³¹ L. E. Helseth, P. E. Goa, H. Hauglin, M. Baziljevich, and T. H. Johansen, *Phys. Rev. B* **65**, 132514 (2002).
- ³² E. H. Brandt, *Phys. Rev. Lett.* **74**, 3025 (1995).
- ³³ T. H. Johansen, M. Baziljevich, H. Bratsberg, Y. Galperin, P. E. Lindelof, Y. Shen, and P. Vase, *Phys. Rev. B* **54**, 16264 (1996).
- ³⁴ Ch. Jooss, J. Albrecht, H. Kuhn, S. Leonhardt, and H. Kronmüller, *Rep. Prog. Phys.* **65**, 651 (2002).